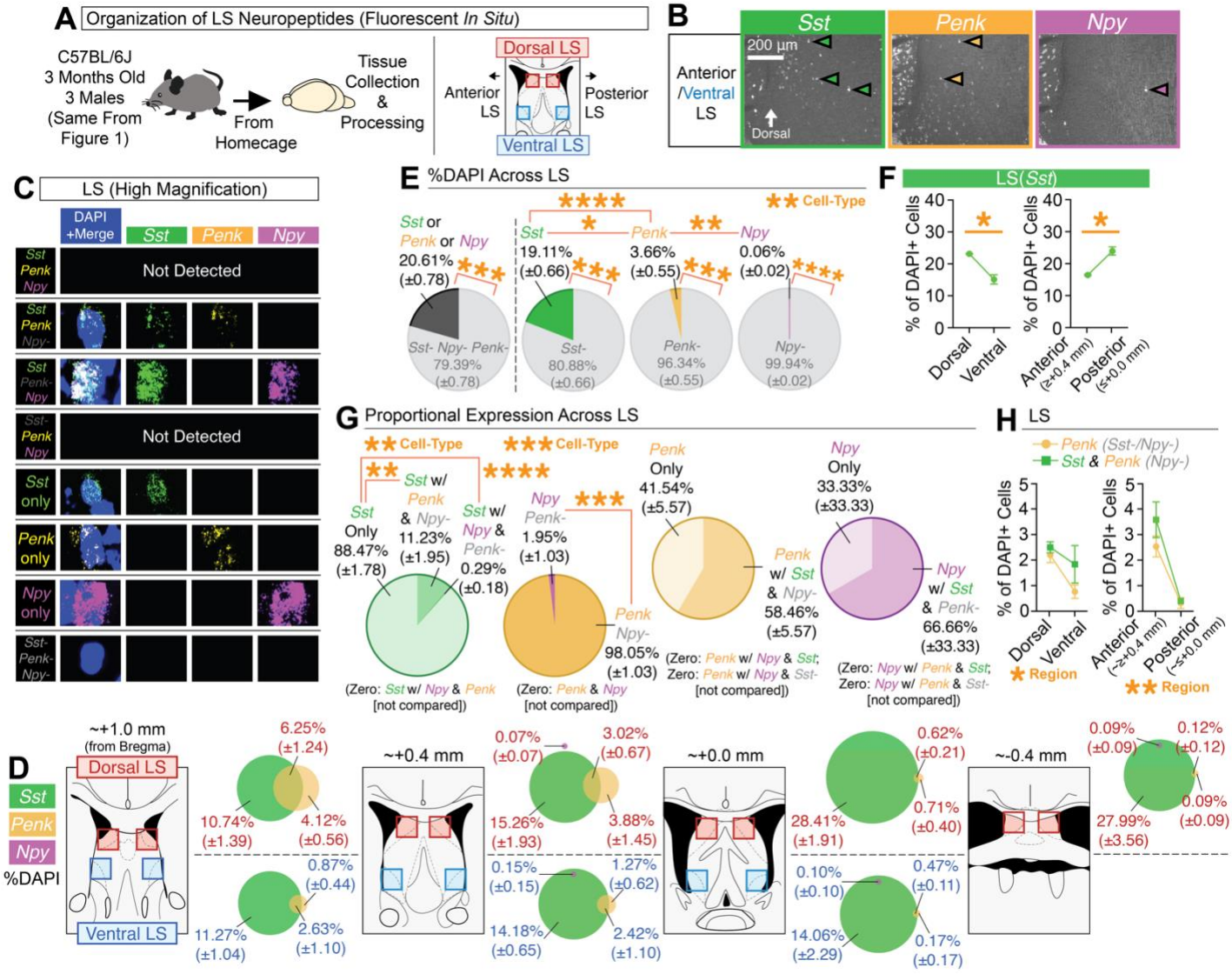

Figure S1 (Related to Main Figure 1). Topographic mapping of neuropeptides reveals partial overlap of *Penk* and *Sst*, whereas *Npy* is sparsely expressed in the LS

(A) Multiplex fluorescent *in situ* hybridization was used to map the neuropeptides *Sst*, *Penk*, and *Npy* in the LS across its dorsal-ventral and anterior-posterior regions. **(B)** Representative coronal images of *in situs* for *Sst*, *Penk*, and *Npy* at different regions of the LS. **(C)** High magnification representative images of individual cells for each of the different cell-types detected for *Sst*, *Penk*, and/or *Npy*. **(D)** Mouse atlas images and venn diagrams [%DAPI (±SEM)] depicting the extent of overlap of *Sst*, *Penk*, and/or *Npy* at each quantified region in the LS. **(E)** Average expression (%DAPI) of *Sst*, *Penk*, and/or *Npy* across all quantified regions of the LS. Main effect of cell-type (ANOVA; significant Tukey's post-hocs) for comparisons of *Sst*-positive, *Penk*-positive, and *Npy*-positive cells. Significant paired t-tests denote comparisons of positive vs. negative expression for each cell-type. **(F)** Average expression (%DAPI) of *Sst* in the dorsal vs. ventral LS and anterior vs. posterior LS (significant paired t-test). **(G)** The average proportion (derived from %DAPI) of each subtype across all quantified LS regions for all *Sst*, *Penk*, and/or *Npy* cells (ANOVA: main effect of cell-type; significant Tukey's post-hocs), all Penk or Npy cells (significant paired t-test), all *Penk* cells with and without *Sst*, and all *Npy* cells with and without *Sst*. **(H)** Comparisons of the average expression (%DAPI) of *Penk* cells with and without *Sst* in the dorsal vs. ventral and anterior vs. posterior regions of the LS (ANOVAs: main effects for region). For the entire figure, all data are shown as mean (±SEM), and for all statistics: *=$p<0.05$; **$p<0.005$, ***$p<0.0005$; ****$p<0.00005$.

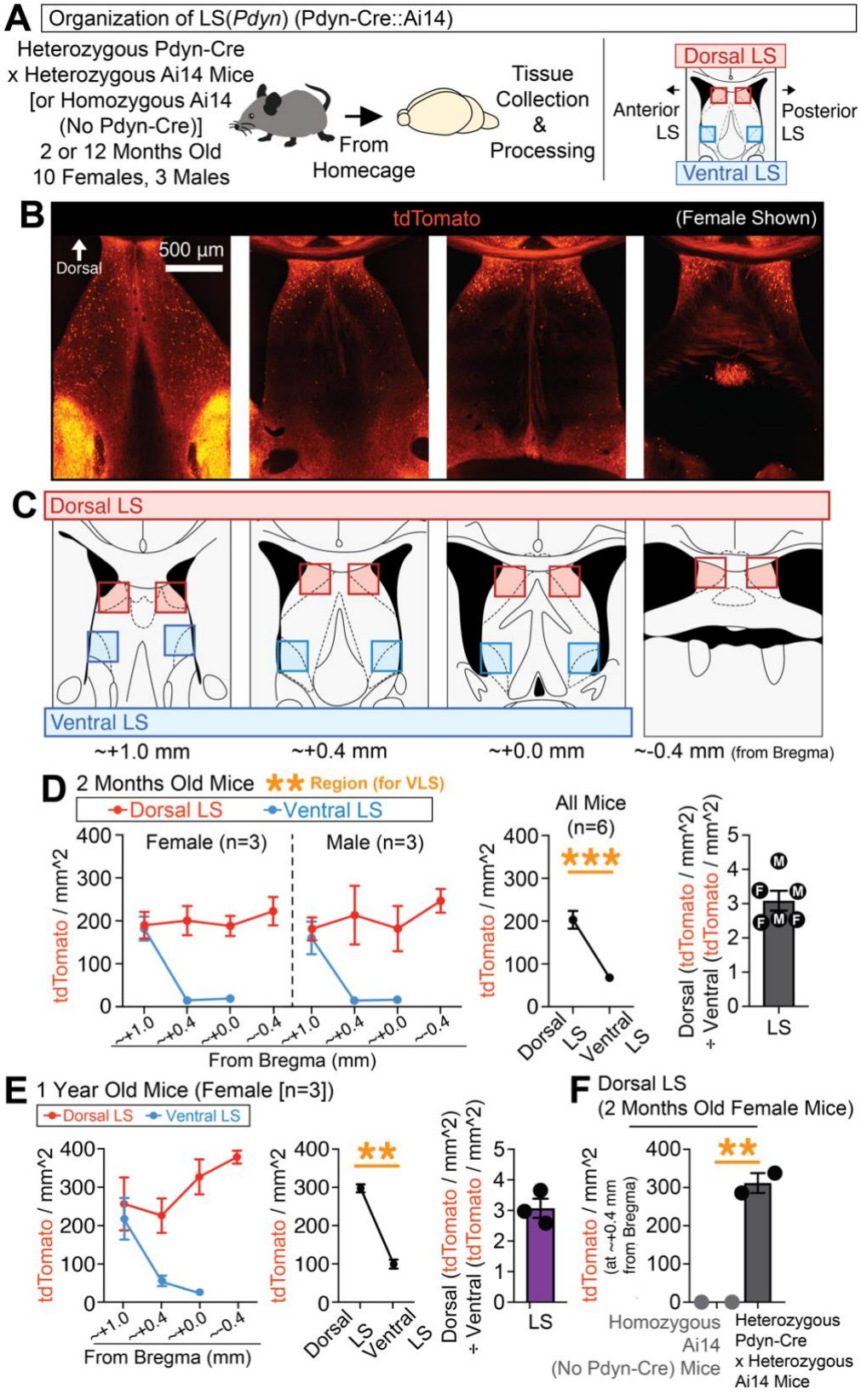

Figure S2 (Related to Main Figure 1). Dorsal bias of developmentally tagged *Pdyn*-expressing cells in the lateral septum of male and female mice

(A) Pdyn-Cre mice were crossed with the Cre-dependent tdTomato-expressing Ai14 reporter line to label and quantify *Pdyn*-expressing cells throughout development in their progeny. **(B)** Representative coronal images of tdTomato-expressing cells in the septum of a Pdyn-Cre::Ai14 mouse. **(C)** Mouse atlas images for regions quantified for tdTomato-labeled cells across the LS. **(D)** Quantification of the number of tdTomato cells (per mm^2) per LS region for 2 months old males and females (left panel), as well as the average number of tdTomato cells across the dorsal vs. ventral regions of the LS (middle panel; significant paired t-test). The rightmost graph depicts the average number of dorsal cells divided by the number of ventral cells for all the mice. **(E)** In female mice aged to 1 year, tdTomato cells were quantified across LS subregions (left panel) and compared for average expression across its dorsal and ventral regions (middle panel; significant paired t-test). The rightmost graph depicts the average number of dorsal cells divided by the number of ventral cells for all the mice. **(F)** Comparisons of the number of tdTomato cells in the posterior-dorsal LS in Ai14-positive (Pdyn-Cre-negative) vs. Pdyn-Cre::Ai14 crosses (significant unpaired t-test). For the entire figure, all data are shown as mean (±SEM), and for all statistics: *=p<0.05; **p<0.005, ***p<0.0005; ****p<0.00005.

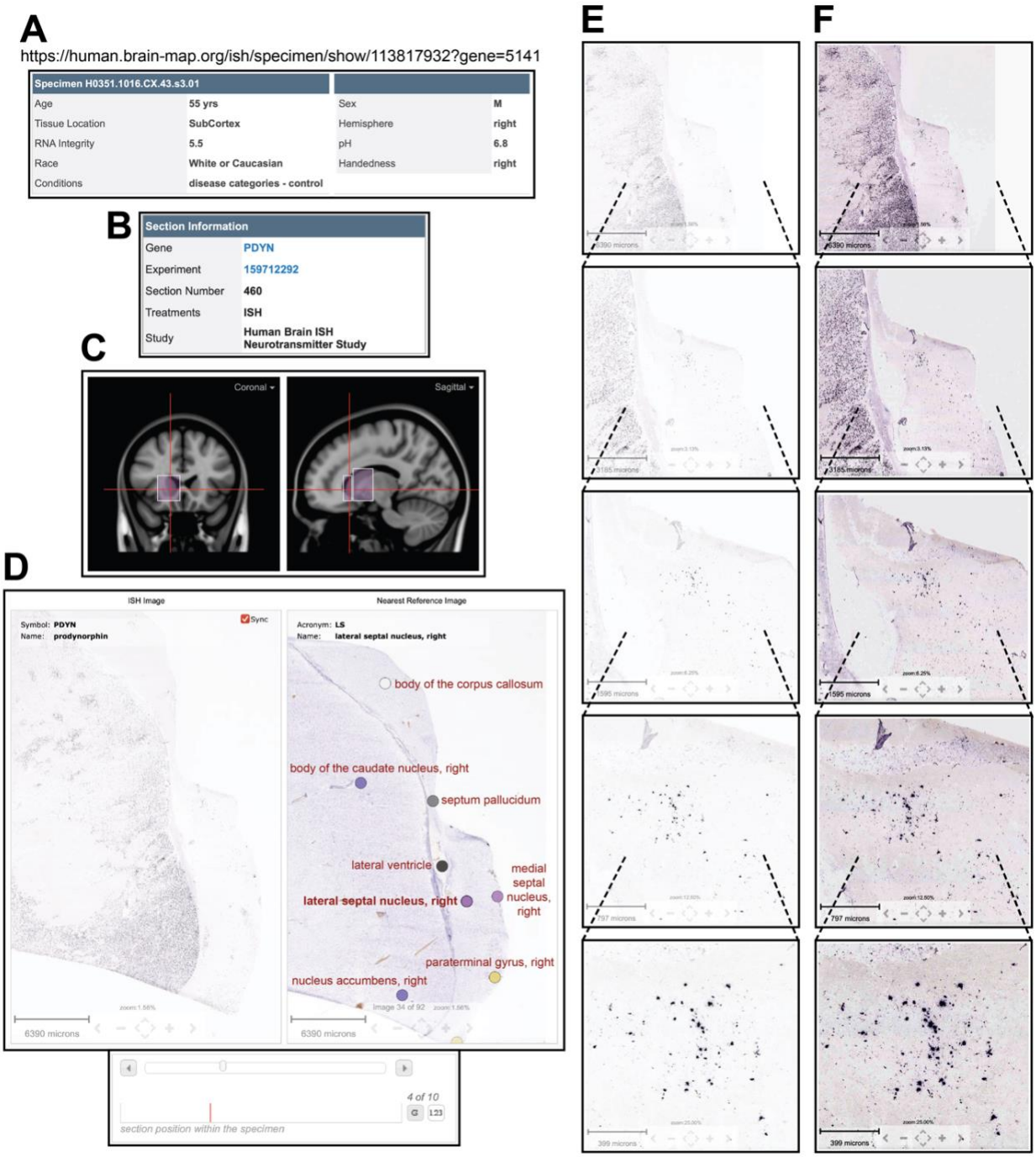

Figure S3 (Related to Main Figure 1). Evidence for conservation of *Pdyn*-expressing cells in the human dorsolateral septum

(A) The website link used and a screenshot of the specimen info for *Pdyn* expression in human brain tissue, accessed from the publicly available Human Brain ISH Neurotransmitter Study from the Allen Brain Institute. All images in this figure are screenshots captured directly from this website. **(B)** Screenshot of section information for tissue shown. **(C)** Screenshot of the approximate coronal/sagittal location of tissue shown. **(D)** Screenshots of an *in situ* for *Pdyn* in the human septum and neighboring structures (left panel), with the labeling of the brain structures noted in the Nissl-stained reference image (right panel). The specific image number in the series of *in situ* images is noted in the screenshot in the bottom panel. **(E)** Screenshots of increasing zoom factor (scale bars included) showing Pdyn expression in the human dorsolateral septum of the same section shown in **(D)**. **(F)** The same images from **(E)** but with the contrast artificially enhanced.

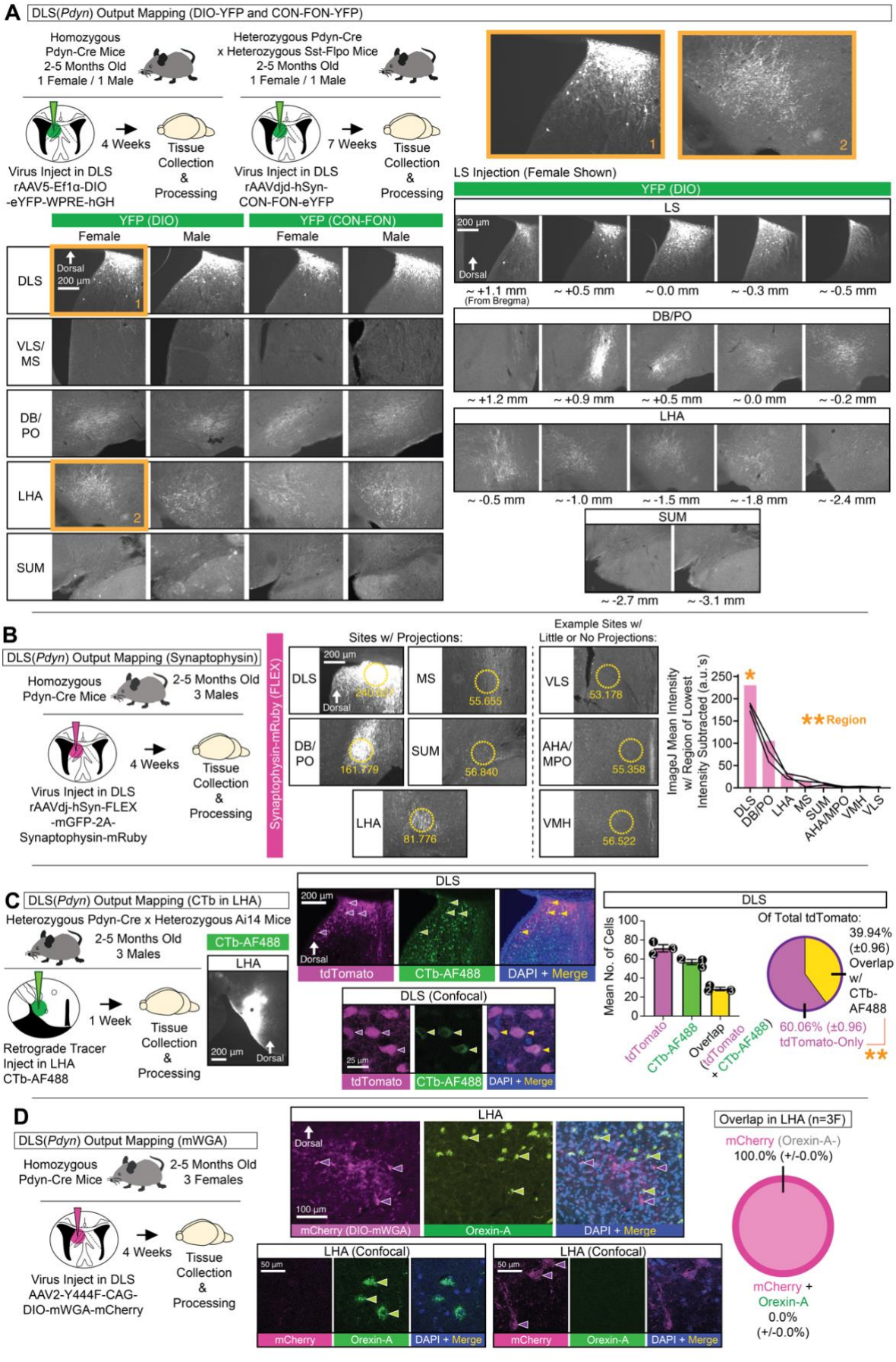

Figure S4 (Related to Main Figure 3). Additional characterization of DLS(*Pdyn*) outputs
(A) Pdyn-Cre or Pdyn-Cre::Sst-Flpo mice were injected in the DLS with Cre-dependent or Cre- and Flpo-dependent (CON-FON) YFP-expressing viruses, respectively. Representative coronal images depict YFP expression in DLS(*Pdyn*) cells and their efferent targets in male and female mice. **(B)** Pdyn-Cre mice were injected in the DLS with Synaptophysin-mRuby-expressing virus. Representative coronal images depict Synaptophysin-mRuby expression in DLS(*Pdyn*) cells and their efferent targets and neighboring targets with little or no expression. Dotted-line circles depict example sites and values for measures of intensity in ImageJ (NIH). Rightmost graph plots mean intensity values for each mouse, with the value from the region of lowest intensity subtracted (ANOVA, main effect of region; significant Bonferroni post-hocs). **(C)** Pdyn-Cre::Ai14 mice were injected in the LHA with the retrograde tracer, CTb-AF488. Representative coronal images show expression of tdTomato and CTb-488 in the DLS of Pdyn-Cre::Ai14 mice. Representative confocal image noting overlap of tdTomato with CTb-488 in the DLS. Rightmost graphs show quantifications of the number of tdTomato- and CTb-AF488-expressing cells (no statistical tests used) and their extent of overlap (pie chart: significant paired t-test). **(D)** Pdyn-Cre mice were injected in the DLS with Cre-dependent anterograde virus (DIO-mWGA-mCherry). Representative coronal images show expression of mCherry and Orexin-A in the LHA. Representative confocal images non-overlapping expression of mCherry and Orexin-A, with the rightmost graph showing quantification of this overlap (pie chart: no statistical tests used).

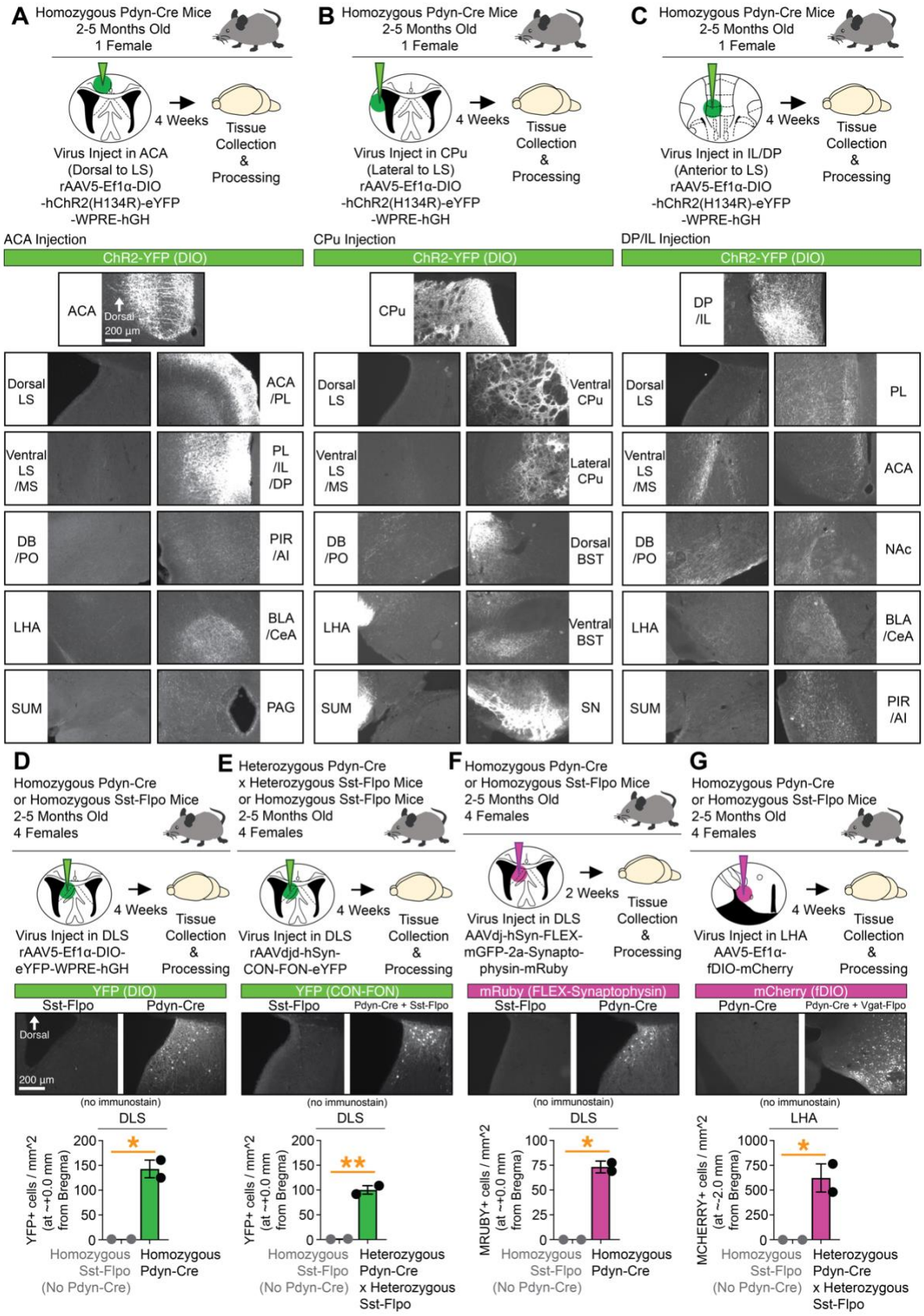

Figure S5 (Related to Main Figure 3). Outputs of DLS-adjacent *Pdyn*-expressing cells and verification of genetic-specificity of viruses

(A) Cre-dependent ChR2-YFP-expressing virus was injected into the ACA directly above the DLS in a Pdyn-Cre mouse. Representative images of the injection site, and example sites of output fibers observed are shown (righthand images), along with sites we previously found DLS(*Pdyn*) projections (lefthand images). **(B)** Cre-dependent ChR2-YFP-expressing virus was injected into the CPu directly lateral to the DLS in a Pdyn-Cre mouse. Representative images of the injection site, and example sites of output fibers observed are shown (righthand images), along with sites we previously found DLS(*Pdyn*) projections (lefthand images). **(C)** Cre-dependent ChR2-YFP-expressing virus was injected into the DP/IL directly anterior to the DLS in a Pdyn-Cre mouse. Representative images of the injection site, and example sites of output fibers observed are shown (righthand images), along with sites we previously found DLS(*Pdyn*) projections (lefthand images). **(D)** Specificity of DIO-YFP expression in the DLS was compared in Sst-Flpo vs. Pdyn-Cre mice (significant unpaired t-test). **(E)** Specificity of CON-FON-YFP expression in the DLS was compared in Sst-Flpo vs. Pdyn-Cre::Sst-Flpo mice (significant unpaired t-test). **(F)** Specificity of FLEX-Synaptophysin-mRuby expression in the DLS was compared in Sst-Flpo vs. Pdyn-Cre mice (significant unpaired t-test). **(G)** Specificity of fDIO-mCherry expression in the LHA was compared in Pdyn-Cre vs. Pdyn-Cre::Vgat-Flpo mice (significant unpaired t-test).

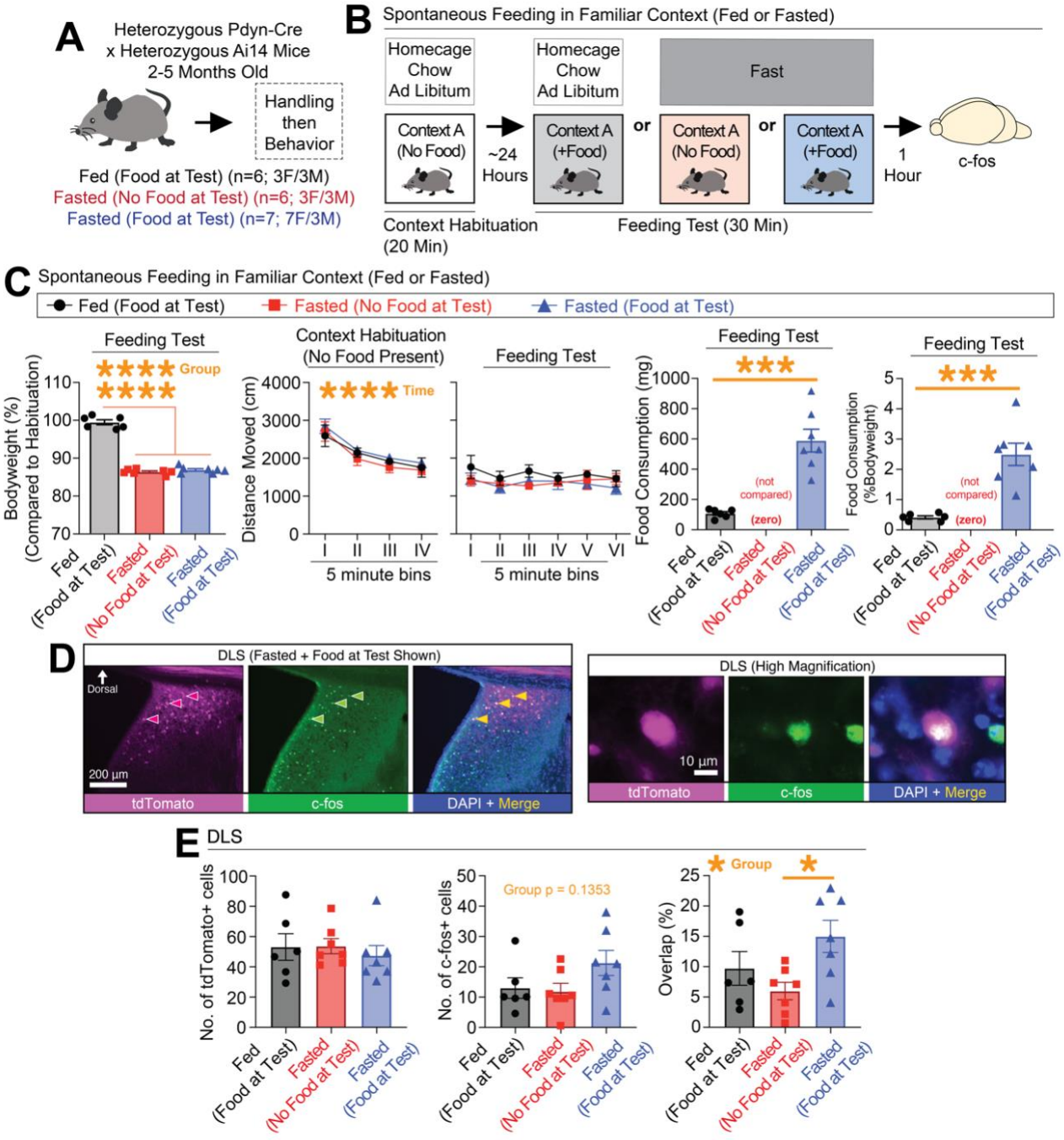

Figure S6 (Related to Main Figure 4). Expression of the immediate early gene, c-Fos, was increased in Pdyn-labeled cells in fasted mice that had access to chocolate flavored food

(**A**) Pdyn-Cre::Ai14 mice were split into three groups. (**B**) Schematic of the behavioral paradigm in which mice were habituated to a context, then either remained on homecage chow or were fasted then given access (or not) to chocolate flavored food in the habituated context. Mice were then sacrificed 1 hour after and processed for c-Fos in the DLS. (**C**) Bodyweight percentages at test, distance moved during each phase (cm), and consumption (mg and %Bodyweight) at test. (**D**) Representative coronal and high-magnification images of c-Fos in the DLS Pdyn-Cre::Ai14 mice that fasted and given food at test. (**E**) Numbers of tdTomato-, c-Fos-expressing, and their overlap (ANOVA, main effect of group, followed by significant Tukey's post-hocs) in the DLS across groups. For the entire figure, all data are shown as mean (±SEM), and for all statistics: *=$p<0.05$; **$p<0.005$, ***$p<0.0005$; ****$p<0.00005$.

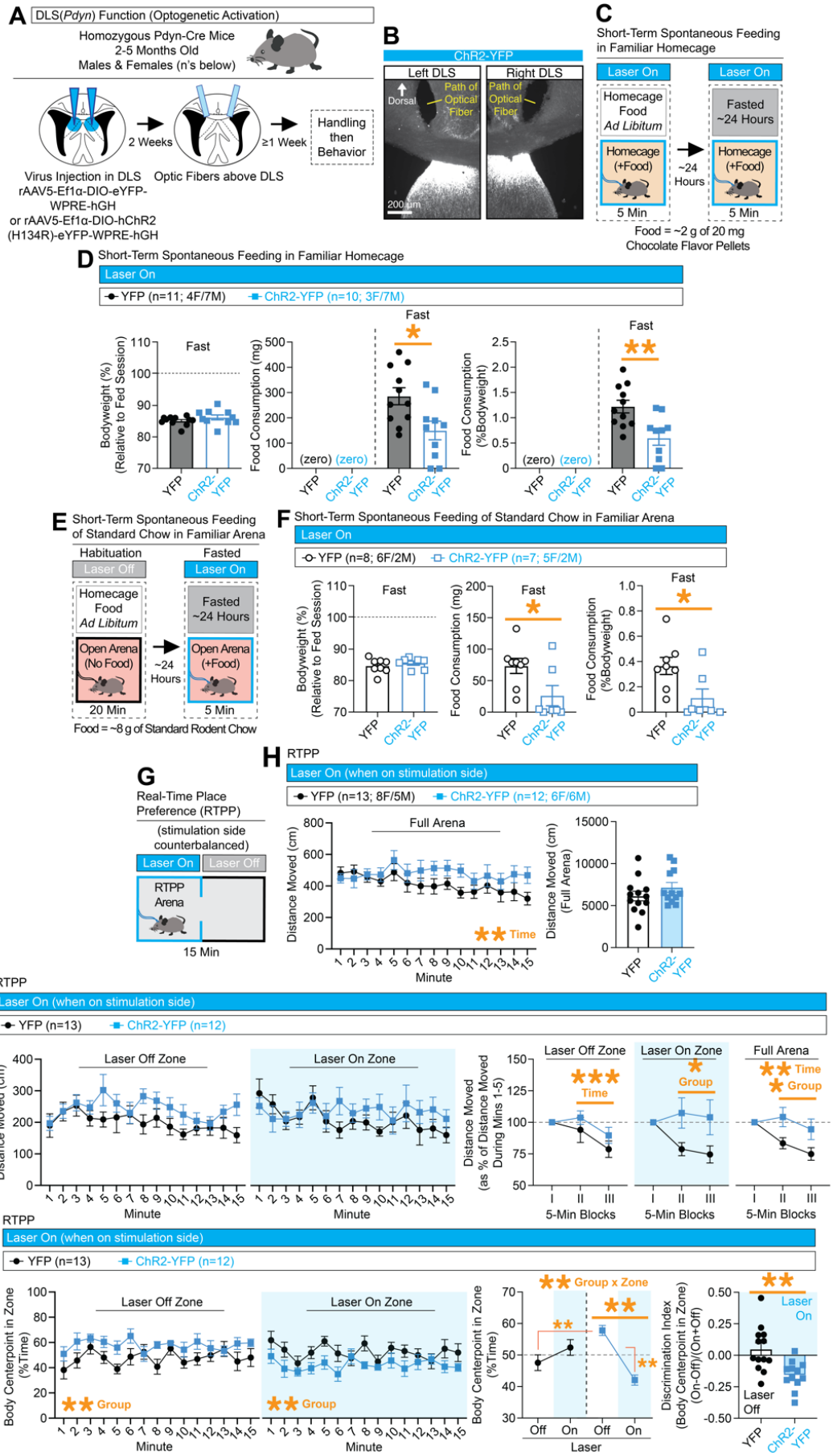

Figure S7 (Related to Main Figure 4). Artificial activation of DLS(*Pdyn*) cells reduces feeding and triggers avoidance

(A) Pdyn-Cre mice were injected with Cre-dependent ChR2-expressing or control virus in the DLS and optic fibers were placed above the DLS. **(B)** Representative coronal images with ChR2-YFP expression in the DLS and optic tracts above the DLS. **(C)** Behavioral design for tests for short-term state-dependent spontaneous feeding in the homecage with optogenetic activation. **(D)** Left graph shows bodyweight (%) relative to the first feeding session. Middle and rightmost graphs show the amount of food consumed (in mg and %Bodyweight) during the *ad libitum* and fasted sessions (significant unpaired t-tests for mg or %Bodyweight during fasted session). **(E)** Behavioral design for testing for short-term spontaneous feeding of regular chow in fasted mice in a familiar arena with optogenetic activation. **(F)** Left graph shows bodyweight (%) at the time of the fasted test relative to the day before. Middle and rightmost graphs show the amount of regular chow consumed (in mg and %Bodyweight) during the fasted test (significant unpaired t-tests for mg or %Bodyweight). **(G)** Behavioral design for real-time place preference (RTPP) with optogenetic activation of DLS(*Pdyn*) cells. **(H)** Distance moved at each minute (left graph; ANOVA, main effect of time) and total distance moved (right) during the full test. (I) Leeft graphs show the distance moved per minute in the laser off and on zones. The final graphs show distance moved as a % of the first 5-min block in the laser off zone (repeated measure ANOVA, main effect of time), in the laser on zone (ANOVA, main effect of group), and for the full arena (ANOVA, main effects of time and group). **(J)** Left graphs show %Time per min in the laser off (ANOVA, main effect of group) and laser on zones (ANOVA, main effect of group). Middle graphs show mean %Time in each zone per group across the test (ANOVA, significant zone x group interaction, significant Bonferroni post-hoc for comparing off vs. on zones in ChR2 mice). A discrimination index was generated based on zone preference at test (significant unpaired t-test). For the entire figure, all data are shown as mean (±SEM), and for all statistics: *=$p<0.05$; **$p<0.005$, ***$p<0.0005$; ****$p<0.00005$.

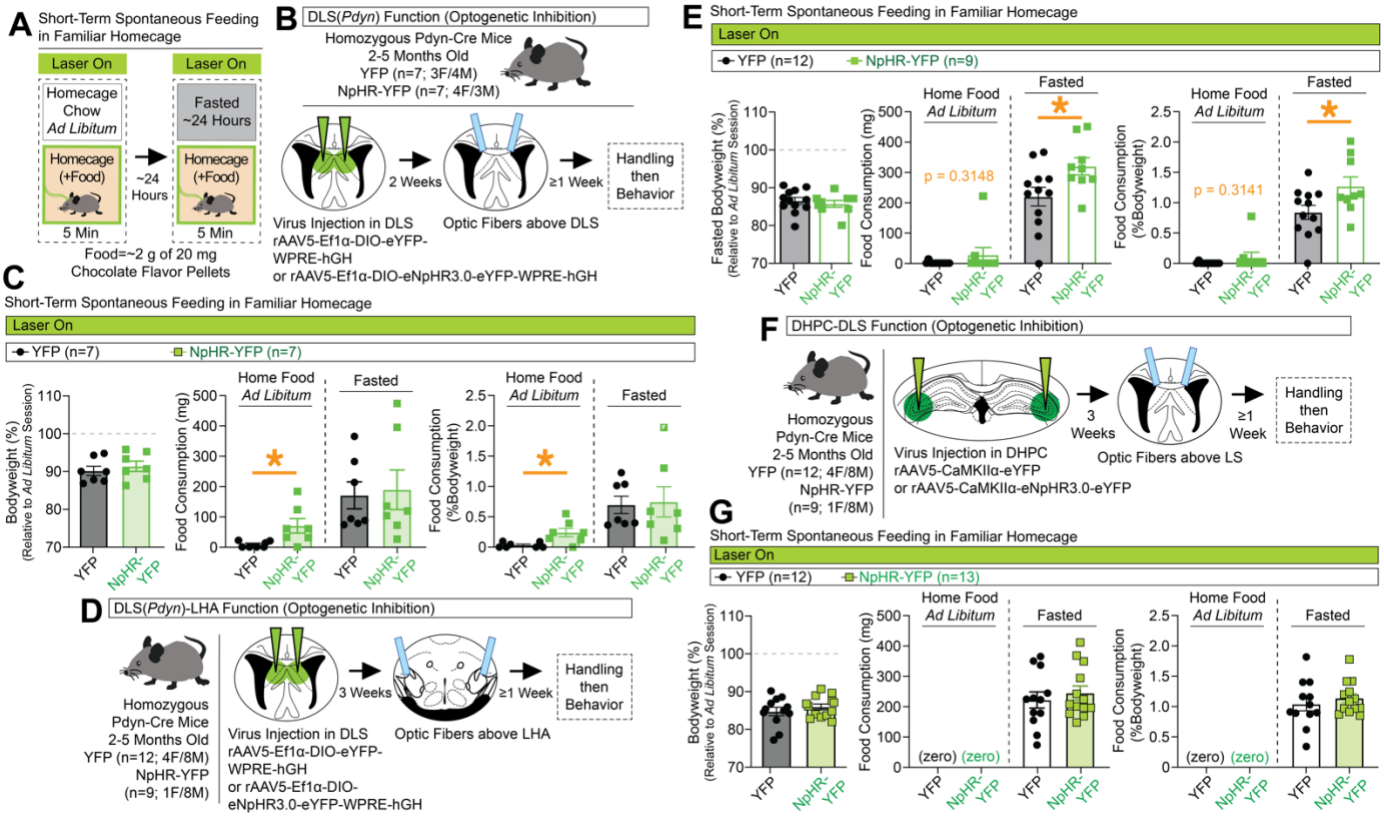

Figure S8 (Related to Main Figure 4). Increases in short-term spontaneous homecage feeding with inhibition of either DLS(*Pdyn*) cells or DLS(*Pdyn*)-LHA terminals, but no changes with DHPC-DLS inhibition

(A) Behavioral design for tests for short-term state-dependent spontaneous feeding in the homecage with optogenetic inhibition. **(B)** Pdyn-Cre mice were injected with Cre-dependent NpHR-expressing or control virus in the DLS and optic fibers were placed above the DLS. **(C)** Left graph shows bodyweight (%) relative to the first feeding session. Middle and rightmost graphs show the amount of food consumed (in mg and %Bodyweight) during the *ad libitum* and fasted sessions (significant unpaired t-tests for mg or %Bodyweight during *ad libitum* session). **(D)** Pdyn-Cre mice were injected with Cre-dependent NpHR-expressing or control virus in the DLS and optic fibers were placed above the LHA. **(E)** Left graph shows bodyweight (%) at the time of the fasted test relative to the day before. Middle and rightmost graphs show the amount of food consumed (in mg and %Bodyweight) during the ad libitum and fasted sessions (significant unpaired t-tests for mg or %Bodyweight during the fasted session). **(F)** Pdyn-Cre mice were injected with NpHR-expressing or control virus in the DHPC and optic fibers were placed above the DLS. **(G)** Left graph shows bodyweight (%) relative to the first feeding session. Middle and rightmost graphs show the amount of food consumed (in mg and %Bodyweight) during the *ad libitum* and fasted sessions. For the entire figure, all data are shown as mean (±SEM), and for all statistics: *=$p<0.05$; **$p<0.005$, ***$p<0.0005$; ****$p<0.00005$.

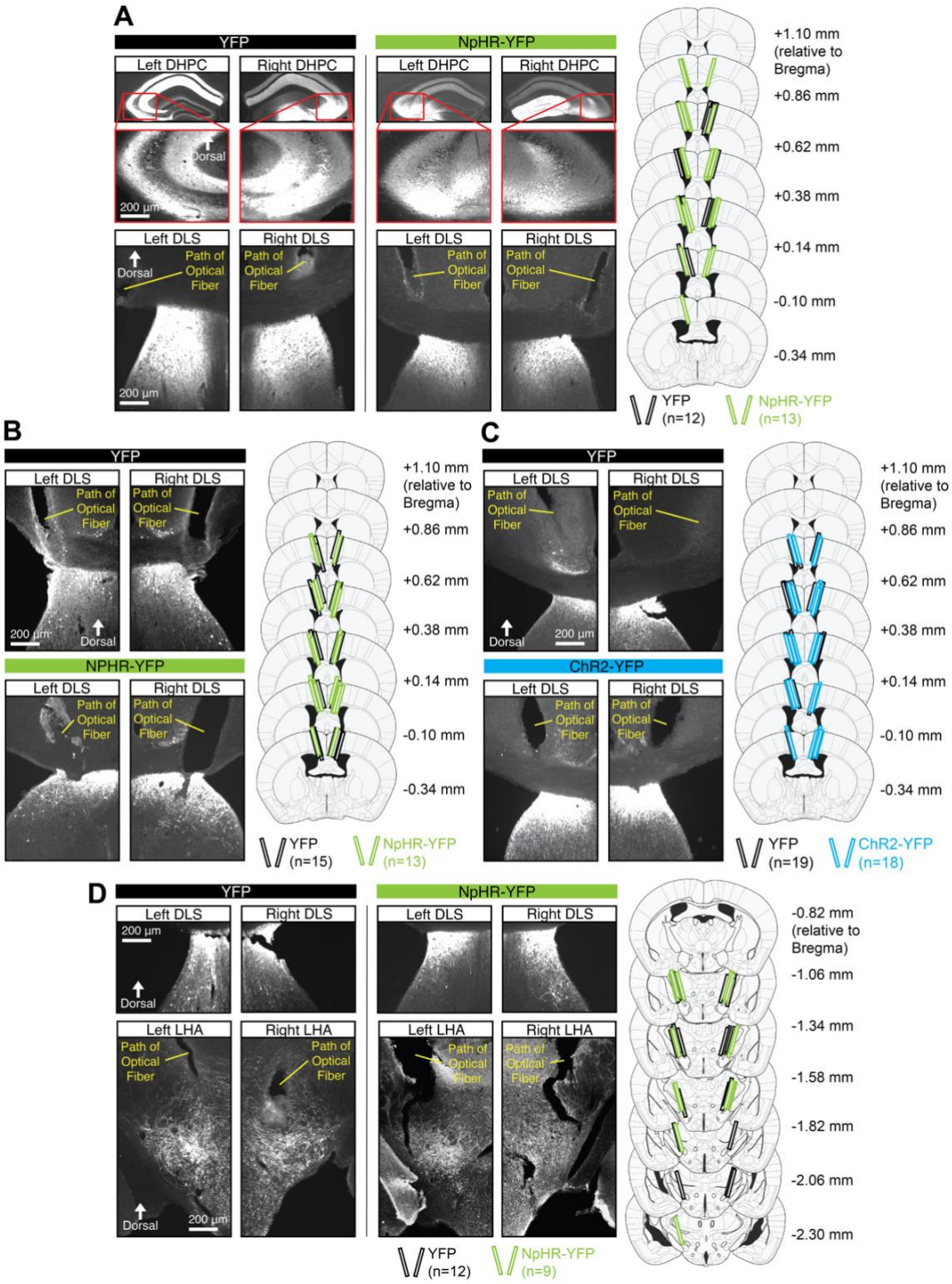

Figure S9 (Related to Main Figure 4). Representative images of viral expression and documentation of placements for optic fibers for behavioral experiments

(A) Representative coronal images of bilateral DHPC and DLS showing viral expression of NpHR-YFP or control virus, as well as optic fiber tracts above the DLS. Modified brain atlas images document placements of optic fibers for each group across all DHPC-DLS optical inhibition experiments. **(B)** Representative coronal images of bilateral DLS showing viral expression of NpHR-YFP or control virus, as well as optic fiber tracts above the DLS. Modified atlas images document placements of optic fibers for each group across all DLS(*Pdyn*) optical inhibition experiments. **(C)** Representative coronal images of bilateral DLS showing viral expression of ChR2-YFP or control virus, as well as optic fiber tracts above the DLS. Modified atlas images document placements of optic fibers for each group across all DLS(*Pdyn*) optical excitation experiments. **(D)** Representative coronal images of bilateral DLS and LHA showing viral expression of NpHR-YFP or control virus, as well as optic fiber tracts above the LHA. Modified atlas images document placements of optic fibers for each group across all DLS(*Pdyn*)-LHA optical inhibition experiments.

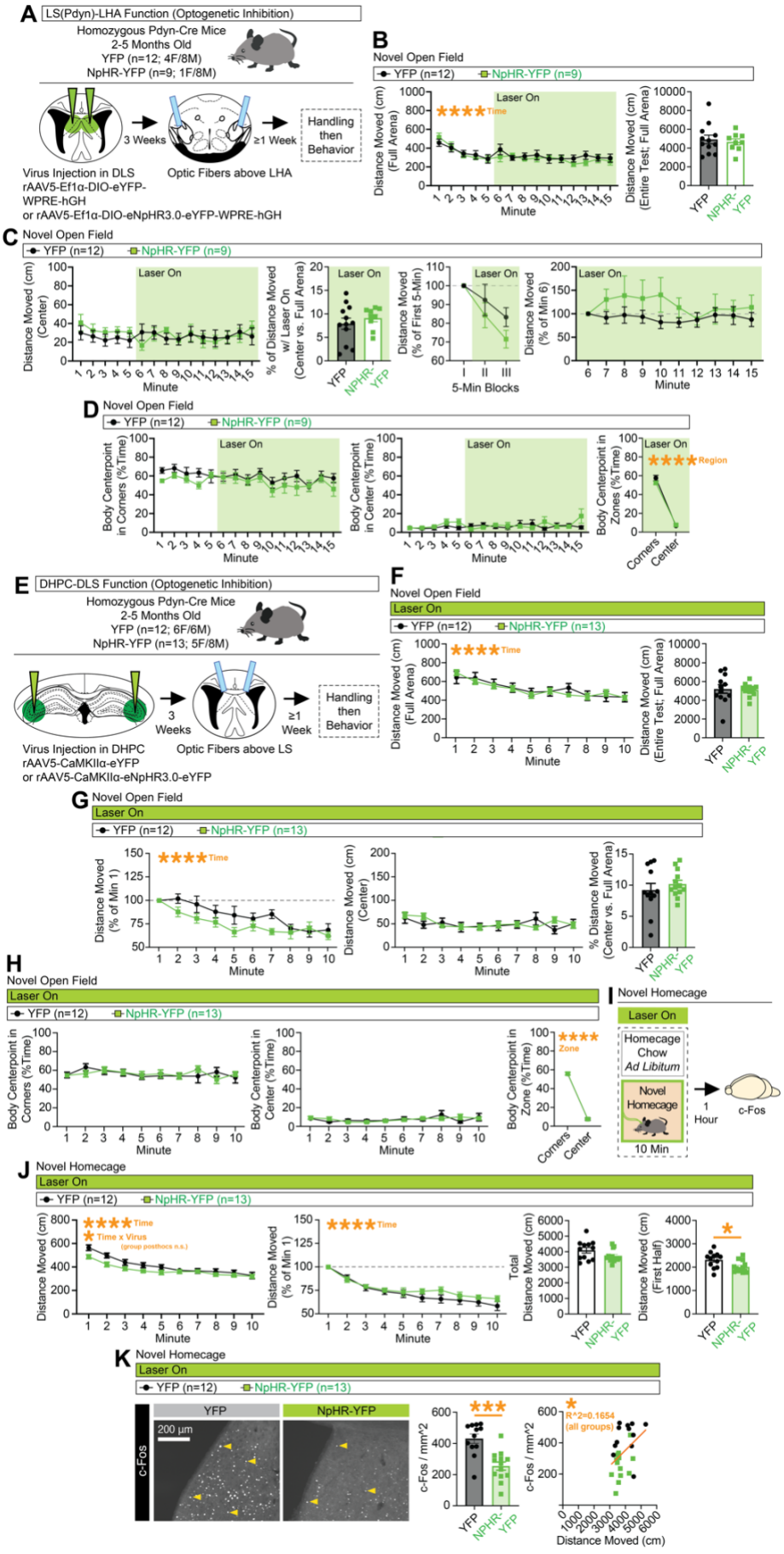

Figure S10 (Related to Main Figure 6). Minimal changes in locomotion or anxiety-like behaviors with optogenetic inhibition of DLS(*Pdyn*)-LHA terminals or DHPC-DLS terminals

(A) Pdyn-Cre mice were injected with Cre-dependent NpHR-expressing or control virus in the DLS and optic fibers were placed above the LHA. Mice were tested for locomotion in a novel open field (15 min) with onset of optical inhibition after 5 min. **(B)** Distance moved (cm) in the full arena of the novel open field during each minute (left graph; ANOVA, main effect of time) and total distance moved at test (right graph). **(C)** Distance moved (cm) in the center of the open field during each minute (left graph). Next graph shows the % of total distance that occurred in the center of the arena, followed by a graph showing distance moved in 5-min blocks as a percent of the first 5-min block. The final graph shows distance moved as a percent of movement during minute 6 for each subsequent minute. **(D)** The percent of time the animal spent in any given corner (left graph) or center (middle graph) of the arena for each minute of the test. Final graph compares time spent in the corners vs. center for full duration of the laser on (ANOVA, main effect of zone). **(E)** Pdyn-Cre mice were injected with NpHR-expressing or control virus in the DHPC and optic fibers were placed above the DLS. Mice were tested for locomotion in an open field and novel homecage. **(F)** Distance moved (cm) in the full arena of the novel open field during each minute (left graph) and total distance moved at test (right graph). **(G)** Distance moved as a % of the first minute for each minute of the test (left graph; ANOVA, main effect of time). Middle graph shows distance moved (cm) in the center of open field. Final graph shows the % of total distance that occurred in the center of the arena. **(H)** The % of time the animal spent in any given corner (left graph) or center (middle graph) of the arena for each minute of the test. Final graph compares time spent in the corners vs. center for the entire test (ANOVA, main effect of zone). **(I)** These same DHPC-DLS mice were exposed to a novel homecage before being sacrificed for c-Fos. **(J)** Distance moved (cm) in the full homecage during each minute (left graph; ANOVA, main effect of time, time x virus interaction). Next graph shows distance moved as a % of the first minute for each minute of the test (ANOVA, main effect of time). Final two graphs show distance moved during the whole test or first 5 min (significant unpaired t-test). (**K**) Representative coronal images showing c-Fos expression in the DLS of NpHR-expressing and control mice (left), this expression quantified (middle; significant unpaired t-test), and the correlation of c-Fos with distance moved across the test (significant R^2, across groups). For the entire figure, all data are shown as mean (±SEM), and for all statistics: *=p<0.05; **p<0.005, ***p<0.0005; ****p<0.00005.